

Cavity Quantum Electrodynamic Enhancement of Stimulated Emission in Microdroplets

A. J. Campillo, J. D. Eversole,^(a) and H-B. Lin

Naval Research Laboratory, Laser Physics Branch, Code 6546, Washington, D.C. 20375

(Received 26 December 1990)

Cavity-QED-enhanced stimulated visible emission was observed in 14- μm -diam rhodamine-6G-ethanol droplets pumped by cw 514.5-nm radiation. Use of droplets provides an excellent test of cavity QED theory for spherical geometries. The mode number and order of the spherical-cavity resonances responsible for the observed emission peaks were identified and their Q values calculated from Lorenz-Mie theory. By equating stimulated gain to calculated/measured cavity losses, it was determined that spherical-cavity Q 's of only 10^3 – 10^4 lead to cavity QED enhancements in excess of 120 in the emission cross section of rhodamine 6G, consistent with theory.

PACS numbers: 42.50.Wm, 12.20.Fv, 32.80.–t, 42.55.–f

It is now generally accepted that the fluorescence from an atom or molecule may be alternatively enhanced [1–3] or inhibited [4,5] by its placement in a microcavity, depending on whether or not the emission spectrally coincides with the cavity resonance. This effect was first discussed by Purcell [1], who noted that the changes in the final density of states per unit volume and unit frequency would lead to a greatly enhanced probability for spontaneous emission over that normally observed in free space. On resonance, the enhancement may be approximated by the expression $3DQ\lambda^3/4\pi^2V_m$, where D is the degeneracy of the resonance, Q is the cavity quality factor, λ is the emission wavelength, and V_m is the mode volume. Much of the previous experimental work on cavity enhancement at visible wavelengths was performed using Fabry-Pérot cavities [6]. Recently, the importance of restricted dimensionality of the cavity, leading to greater spontaneous emission rates [7], was noted. A spherical cavity represents a case of three-dimensional enclosure and is attractive because all fields and modes, both internal to and external to the cavity, are exactly calculable in practice. It has been known for some time that nearly transparent microdroplets act as such high- Q resonators, the feedback provided by light waves that totally internally reflect at the droplet-air interface and fold back on themselves [8]. Spherical-cavity resonances in micrometer-sized droplets occur at a series of discrete wavelengths throughout the visible. For a given droplet, resonances occur at specific values of $x_{n,l}$. Here x is the size parameter given by $2\pi a/\lambda$, where a is the droplet radius, and n and l are integers. The mode number n indicates the order of the spherical Bessel and Hankel functions describing the radial field distribution and the order l indicates the number of maxima in the radial dependence of the internal field distribution. Both discrete transverse electric (TE) and transverse magnetic (TM) resonances exist. Emission from dielectric microspheres [9] and fibers [10] containing fluorescing dyes shows sharp line structure superimposed on the normal broadband emission. These spectral features (see Fig. 1) result from cavity quantum electrodynamic (QED) enhancement of the Einstein A coefficient at specific spherical-cavity-reso-

nance wavelengths. Recent theoretical work [11–13] predicts very large (200–1500 times) cavity QED enhancements in the A coefficient of molecules embedded in such micrometer-sized droplets. It has not been previously possible to perform quantitative experiments on such droplets owing to the inability of identifying the specific mode number and order of the many observed resonances. Each of the modes has dramatically different spatial properties, cavity Q , and consequently, varying degrees of enhancement. In addition, contributions to the total fluorescence from other portions of the droplet not affected by the cavity further complicate the experiment by providing an intense broad spectral background (see Fig. 1). In the present work, we estimate the magnitude of the enhancement by equating lasing gain (related to the B coefficient) to the cavity losses at wavelengths corresponding to various resonant modes. To achieve this, we rely on a newly developed procedure [14] for identifying the participating spherical-cavity resonances. Once identified, the Q of the mode is calculated from Lorenz-Mie theory, as well as measured experimentally from low-intensity linewidth measurements. Using this procedure, we find that Einstein- B -coefficient enhancements of 120 are typical for a relatively low- Q mode (2.6×10^3), consistent with theoretical predictions [11–13].

A vibrating-orifice aerosol generator [15] (VOAG) was used to produce a falling linear stream of virtually identical (less than 2 parts in 10^5 diameter variation), 14- μm -diam droplets of $10^{-5}M$ rhodamine 6G (R6G) in ethanol solution, which were excited (50–600 W/cm^2) by a cw argon-ion laser. Concentration of the dye was verified by measuring the absorption coefficient α of a 1-cm sample at the excitation wavelength (514.5 nm) to be 1.3 cm^{-1} . Previous studies have shown that evaporation of the solvent was negligible under the present operating conditions of the VOAG. Droplet emission was examined using a double 1-m Spex spectrometer and photomultiplier. The sample liquid is direct pressure fed to a 5- μm vibrating orifice. The droplet stream could be calibrated by inducing a size ramp through the use of a frequency synthesizer to drive a piezoelectric transducer mounted on the orifice. Droplet scattered light as a function of VOAG

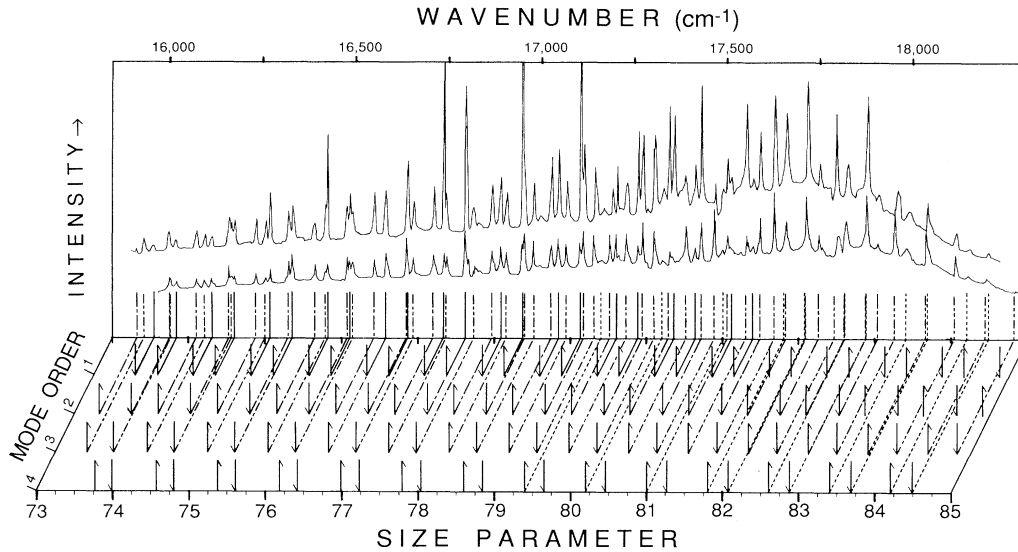


FIG. 1. Emission spectra observed from rhodamine 6G in ethanol droplets (lower and upper curves obtained under 300 and 400 W/cm^2 excitation intensity). The spectral peaks superimposed on the usual broadband dye emission are due to cavity QED enhancement of the emission and their positions correlate well with predicted spherical-cavity-resonance λ 's. Up (down) arrows refer to TE (TM) modes.

frequency was monitored at an angle of 89.9° using both He-Ne (632.8 nm) and argon-ion (514.5 nm) laser light as probes. Following a previously described procedure [14], unique matches to the elastic-scattering data were obtained by comparison to curves calculated from Lorenz-Mie theory. This establishes a precise one-to-one correlation between orifice frequency and droplet size as well as the indices of refraction at 514.5 and 632.8 nm and the calculated placement of cavity resonances.

Figure 1 shows two typical R6G emission spectra from a $7.36\text{-}\mu\text{m}$ -radius droplet as well as the predicted wave-

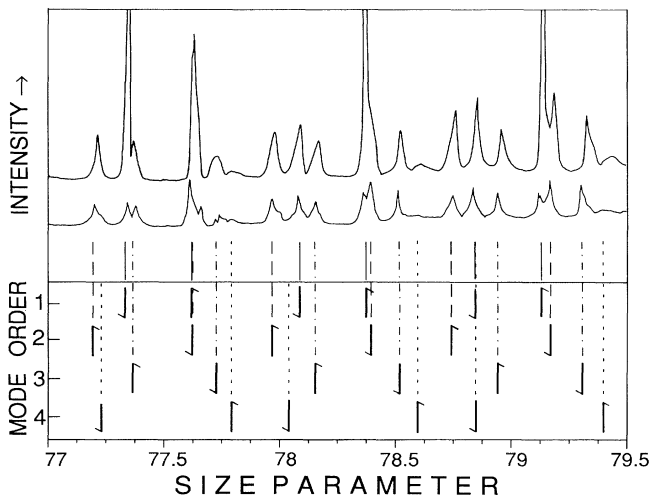


FIG. 2. A magnified portion of Fig. 1 showing the precision of the predicted mode placements.

number and size-parameter placement of all spherical cavity resonances from $l=1$ to 4. Up (down) arrows refer to TE (TM) modes. The positions of the measured and predicted resonances correlate well, as is shown in Fig. 2 which is an expanded portion of Fig. 1. All four mode orders can be seen at various places in the spectrum. The $l=1$ and 2 modes show clear signs of lasing (e.g., nonlinear growth) at our lowest pump intensities ($50 \text{ W}/\text{cm}^2$), whereas the third- and fourth-order modes require higher powers to reach threshold. This behavior is related to the cavity Q of the various modes which can be estimated from elastic-scattering linewidths ($Q = x/\Delta x = \nu/\Delta\nu$) calculated from Lorenz-Mie theory. The total cavity quality factor Q is a measure of the feedback provided by the mode. In Fig. 3, Q_{HS} is calculated using only the *real* part of the refractive index m . The term Q_{ext} is used [14] as a measure of the cavity light leakage (fraction radiated per pass is $2\pi m x/Q_{\text{ext}}$). In general, $1/Q_{\text{ext}} = 1/Q_{\text{HS}} + 1/Q_{\text{pert}}$, where Q_{pert} accounts for the deviation of a real droplet from a homogeneous sphere due to shape and index perturbations. Broadening due to absorption is accounted for by using Q_{abs} , defined as $2\pi m/\lambda\alpha$, in the expression $1/Q = 1/Q_{\text{ext}} + 1/Q_{\text{abs}}$. Generally the $l=1$ and 2 modes are not observed at higher wave numbers, while the third- and fourth-order modes favor this part of the spectrum. The fraction of light eventually coupled out of the droplet compared to that absorbed [14] is given by Q/Q_{ext} . Because of its implicit dependence on α through the dye singlet-state absorption, Q rapidly decreases with increasing wave number, and when $Q/Q_{\text{ext}} \ll 1$ the mode disappears. The lower-order high- Q modes are more sensitive to absorption and are consequently not visible at high wave numbers in Fig. 1.

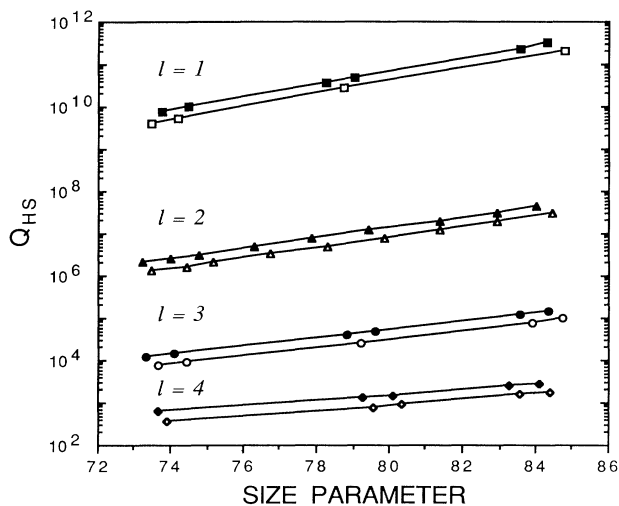


FIG. 3. Cavity Q 's as a function of size parameter calculated from Lorenz-Mie theory. Here, a homogeneous sphere was assumed with $a = 6.82 \mu\text{m}$ and $m = 1.363$, corresponding to ethanol droplets of similar parameters used to obtain the data of Figs. 1 and 2. Squares, triangles, circles, and diamonds refer to modes of order one, two, three, and four, respectively. Solid symbols correspond to TE modes, while open symbols correspond to TM modes.

Q_{pert} may be determined from this behavior by noting when the first-order modes appear spectrally at reduced intensity (e.g., $Q/Q_{\text{ext}} \approx Q_{\text{abs}}/Q_{\text{ext}} \approx 0.1$ at 17600 cm^{-1}). Using a measured value of α at this wavelength, an estimate for Q_{pert} of 10^8 was obtained. Therefore, total Q 's for the first- and second-order modes are lower than the Q_{HS} 's shown in Fig. 3 when the effects of shape perturbations and singlet absorption at short wavelengths are considered. Q 's of $l=1$ modes are typically 10^7 – 10^8 , while those of $l=2$ modes are about 10^6 or less. However, Q 's of the third- and fourth-order modes are approximately equal to the Q_{HS} 's shown.

Figure 4 shows an expanded portion of the emission spectra around 18100 cm^{-1} . Although the excitation intensity has increased by only 50% over the three superimposed spectra shown, the emission intensity of the two features has increased more than sixfold. The existence of such a dramatic nonlinear intensity dependence is a traditional indication that these modes are lasing [16]. At pump intensities lower than those used in Fig. 4, the peak heights of these features show a linear dependence with pump intensity, while at much higher pump levels the data again display a linear dependence but with greater slope. Although Yokoyama and Brorson [16] predict the disappearance of a well-defined threshold in a single-mode microcavity laser, this situation is not applicable in our multimode case. While the presence of lasing $l=1$ and 2 order modes can be nominally explained by the high-cavity Q 's associated with these modes, even assuming a gain calculated from bulk R6G emission cross-section values, our observation that $l=3$ and 4 modes

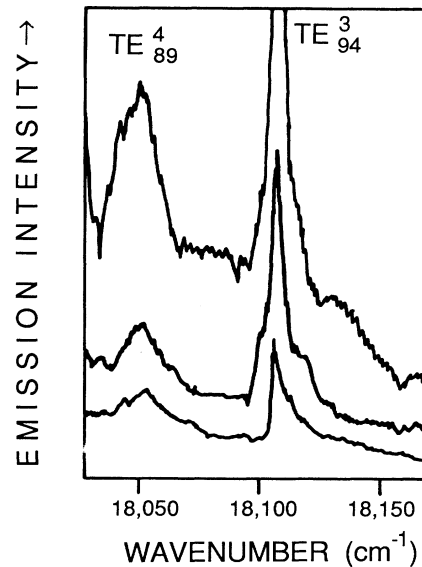


FIG. 4. Nonlinear emission characteristic of two resonant modes just above lasing threshold. Lower, middle, and upper curves were obtained using excitation intensities of 400, 500, and 600 W/cm^2 , respectively.

also lase at R6G molar concentrations of 10^{-5} cannot. These lasing modes are direct evidence of substantial cavity enhancements. Without enhancement, there simply is not enough gain present, even if all R6G molecules present were excited, to compensate for the coupling losses.

One may express the gain per length of a conventional dye laser [17] by the expression

$$g = N_1 \sigma_{\text{em}} - N_0 \sigma_S - N_T \sigma_T, \quad (1)$$

where N_1 , N_0 , and N_T are the populations per volume of excited singlet-state, ground-state, and triplet-state species, respectively. $\sigma_{\text{em}}(\lambda)$, $\sigma_S(\lambda)$, and $\sigma_T(\lambda)$ are the singlet emission cross section, the singlet-state absorption cross section, and the triplet-state absorption cross section, respectively. An upper bound on the microcavity-enhanced gain/length g^c may be obtained by assuming a limiting value of N_1 equal to all R6G molecules present, N :

$$g^c(\lambda) \leq N \sigma_{\text{em}}^c(\lambda). \quad (2)$$

In Eq. (2), the cavity-enhanced cross section σ_{em}^c is assumed to be related to the noncavity value by $\eta = \sigma_{\text{em}}^c / \sigma_{\text{em}}$. For a mode to lase, its gain/length must equal or exceed the cavity transmission losses per length, $2\pi m / \lambda Q$; therefore, its enhancement must satisfy the relation

$$\eta \geq \frac{2\pi m}{\lambda Q N \sigma_{\text{em}}(\lambda)}. \quad (3)$$

The enhancement of the emission cross section discussed

here is in addition to and quite distinct from the strong increase in the low-amplitude spontaneous-emission signal [18] or lasing gain that results from a pump intensity buildup within the droplet cavity. In deriving Eq. (3), we assumed that the pump excitation level is sufficiently high that the gain is saturated and independent of intensity. This is a great simplification as the precise details of the field distribution of the pump within the droplet may be neglected. The right-hand side of Eq. (3) reaches a maximum experimental value which more closely reflects the true magnitude of η when the number of dye molecules has been reduced to the point where the mode under consideration is barely able to sustain lasing.

In the case of the TE_{89}^4 mode shown in Fig. 4, the relevant experimental values are $Q=2600$, $N=5 \times 10^{15}$ molecules/cm³, and $\sigma_{em}=10^{-16}$ cm² at 18100 cm⁻¹ [17]. Using Eq. (3), the experimentally obtained lower bound on η is ca. 120. This number is significantly larger than previously reported [6,19] enhancements in the visible, due in large part to the higher dimensionality of the spherical cavity. If we approximate [13] the mode volume to droplet volume by $1/m^2 D^{1/2}$, where the degeneracy D is given by $2n+1$, it can be shown that Purcell's formula for the droplet case may be written $\eta \approx 9m^2 D^{3/2} Q/2x^3$. On the basis of Purcell's formula, the calculated η for the TE_{89}^4 mode is 90, in agreement with the lasing value to within experimental error. If Purcell's formula were to remain valid at the highest droplet Q 's (ca. 10^8), cavity enhancements in excess of 10^6 would occur. The theory of the high- Q strong-coupling regime [13] has not yet been addressed in the literature for the case of lasing gain and so the validity of Purcell's relation in this regime remains an open question. However, the experimental approach outlined here should begin to provide some answers to this and related questions.

In summary, we have observed large-cavity QED enhancements for spherical resonators (>120) as predicted by theory even though the cavity dimension greatly exceeds the wavelength of visible light. The use of naturally occurring liquid droplet cavities provides an excellent vehicle for confronting cavity QED theory with experiments in regimes that are exactly calculable. Cavity

effects such as Rabi nutations, fluorescence inhibition, and spectral modification should be readily observable as well.

- (a)Also with Potomac Photonics, Inc., Lanham, MD 20706.
- [1] E. M. Purcell, Phys. Rev. **69**, 681 (1946).
 - [2] P. Stehle, Phys. Rev. A **2**, 102 (1970).
 - [3] P. Goy, J. M. Raimond, M. Gross, and S. Haroche, Phys. Rev. Lett. **50**, 1903 (1983).
 - [4] D. Kleppner, Phys. Rev. Lett. **47**, 233 (1981).
 - [5] R. G. Hulet, E. S. Hilfer, and D. Kleppner, Phys. Rev. Lett. **55**, 2137 (1985).
 - [6] F. De Martini, G. Innocenti, G. Jacobovitz, and P. Mataloni, Phys. Rev. Lett. **59**, 2955 (1987); F. De Martini and G. Jacobovitz, Phys. Rev. Lett. **60**, 1711 (1988).
 - [7] S. D. Brorson, H. Yokoyama, and E. P. Ippen, IEEE J. Quantum Electron. **26**, 1492-1499 (1990).
 - [8] S. C. Hill and R. E. Benner, J. Opt. Soc. Am. B **3**, 1509 (1986).
 - [9] R. E. Benner, P. W. Barber, J. F. Owen, and R. K. Chang, Phys. Rev. Lett. **44**, 475 (1980).
 - [10] J. F. Owen, P. W. Barber, P. B. Dorain, and R. K. Chang, Phys. Rev. Lett. **47**, 1075 (1981).
 - [11] H. Chew, Phys. Rev. A **38**, 3410 (1988); **37**, 4107 (1988); J. Chem. Phys. **87**, 1355 (1987).
 - [12] S. C. Ching, H. M. Lai, and K. Young, J. Opt. Soc. Am. B **4**, 1995 (1987); **4**, 2004 (1987).
 - [13] H. M. Lai, P. T. Leung, and K. Young, Phys. Rev. A **37**, 1597 (1988).
 - [14] J. D. Eversole, H-B. Lin, A. L. Huston, and A. J. Campillo, J. Opt. Soc. Am. A **7**, 2159 (1990); H-B. Lin, A. L. Huston, J. D. Eversole, and A. J. Campillo, J. Opt. Soc. Am. B **7**, 2079 (1990).
 - [15] H-B. Lin, J. D. Eversole, and A. J. Campillo, Rev. Sci. Instrum. **61**, 1018 (1990).
 - [16] H. Yokoyama and S. D. Brorson, J. Appl. Phys. **66**, 4801 (1989).
 - [17] B. B. Snavley, in *Dye Lasers*, Topics in Applied Physics Vol. 1, edited by F. P. Schäfer (Springer-Verlag, New York, 1989), pp. 91-137.
 - [18] S. Hayashi, R. Koh, Y. Ichiyama, and K. Yamamoto, Phys. Rev. Lett. **60**, 1085 (1988).
 - [19] D. J. Heinzen, J. J. Childs, J. E. Thomas, and M. S. Feld, Phys. Rev. Lett. **58**, 1320 (1987).